Electrochimica Acta, Vol. 35, No. 2, pp. 489–496, 1990.
Printed in Great Britain.

0013-4686/90 $3.00 + 0.00

THE MECHANISM OF SILVER(I) OXIDE FORMATION ON POLYCRYSTALLINE SILVER IN ALKALINE SOLUTION. DETERMINATION OF NUCLEATION AND GROWTH RATES

C. ALONSO,* R. C. SALVAREZZA,*† J. M. VARA* and A. J. ARVIA‡

*Departamento de Química, Universidad Autónoma de Madrid, 28049 Madrid, Spain

‡INIFTA, Universidad de La Plata, Sucursal 4, Casilla de Correo 16, La Plata, Argentina

(*Received* 1 *March* 1989; *in revised form* 9 *May* 1989)

Abstract—The nucleation and growth of Ag(I) oxide layers on polycrystalline Ag electrodes is studied by potentiodynamic and potentiostatic current transients in 0.1 M NaOH. A model involving the diffusion controlled growth of a basal layer followed by the nucleation and growth of a secondary layer is proposed. Various nucleation parameters are estimated by comparing experimental data with simulated transients, and the results are discussed in terms of the atomistic theory of electrochemical phase formation. The influence of the nucleation parameters on the shape of the current transients is analysed and some controversial results in the literature are explained.

INTRODUCTION

The study of nucleation kinetics involves the evaluation of the steady-state nucleation rate (I_{st})[1], that is the product αN_0, where α denotes the nucleation rate, and N_0 is the number density of active sites on the electrode surface[2]. Usually, nucleation experiments provide information about I_{st} and/or N_s the saturation number of nuclei[3], but not directly N_0 or α. It should be remembered that N_0 and N_s seldom coincide due to the appearance of exclusion zones around growing nuclei. However, a method has been proposed to find out both α and N_0 through the analysis of current transient maxima recorded at a sequence of constant potentials[4]. This method, which although it is based on a great many assumptions and it has been reported to be reliable and self-consistent for mercury electrodeposition on platinum electrodes[5, 6], opens the possibility—if it is correct—of obtaining basic information about electrochemical phase formation.

Recently, it was proposed that the electroformation of Ag(I) oxide layers involves the nucleation and growth of secondary islands on a basal oxide layer[7]. On this basis, the voltammetric current peaks AI, AI′ and AI″ (Fig. 1) that are observed[8, 9] during anodic scans in NaOH solutions can be assigned to the initial electroformation of AgOH monolayer and to a primary oxide layer (layer I), followed by the nucleation and growth of 3-D centers (layer II). Current transients at a constant potential are more complex, however, due to the simultaneous growth of the various layers[7]. Hence, conventional analysis of current maxima to obtain information about the nucleation and growth processes is precluded. Nevertheless, the electrochemical formation of the Ag(I) oxide layer is an interesting process to be analysed in terms of the latest developments in the theory of electrochemical phase formation.

In the present work simulation techniques are used to fit theoretical current transients to experimental data for the potentiostatic electroformation of the Ag(I) oxide layer on polycrystalline silver, the goal being to evaluate the nucleation parameters N_0, α, and I_{st}. These parameters are then discussed in terms of the theory of electrochemical phase formation.

EXPERIMENTAL

The electrochemical arrangement consisted of a polycrystalline (pc) silver electrode (0.05 cm^2 geometric area), a large platinum counter electrode, and a saturated calomel electrode (*sce*) as the reference electrode, each being placed in the usual way in a conventional three compartment glass made cell. Potentials in the text are referred to the *sce* scale. The electrolyte was 0.1 M NaOH.

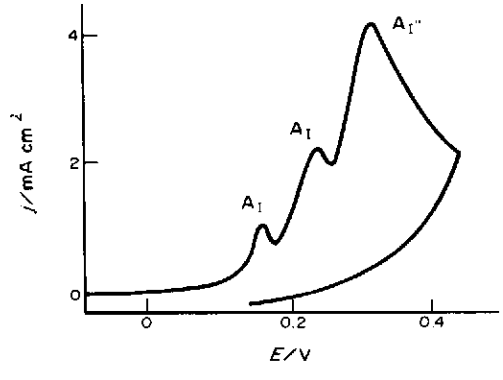

Fig. 1. Current density (j)/potential(E) profile for a polycrystalline Ag electrode run at $v = 0.1$ V s^{-1} between −0.20 and 0.45 V in 0.1 M NaOH.

†Permanent address: INIFTA, La Plata, Argentina.

The kinetics of nucleation were studied at 298 K by means of the potentiostatic step (E_s) technique by recording the corresponding current transients for different E_s values. The perturbing potential programme involved a precathodisation at −1.30 V during 60 s, followed by a potential step during a certain time, t_a, to a value set either at −0.27 V, that is, a potential range which can be assigned to the double layer region or at the potential of peak AI′ (see insert in Fig. 2). Finally, the potential was stepped to the selected E_s value. A complete description of the experimental setup, electrodes and solution preparation, and measurements techniques was presented elsewhere[7].

RESULTS

The current transients shown in Fig. 2 demonstrate that the kinetics of the Ag(I) oxide phase electroformation depends considerably on the electrode pretreatment as well as on the value of the applied potential step, E_s. Thus, a decreasing current transient results by stepping the potential from the double layer region to the potential region of peak AI′ (Fig. 2a; E_s = 0.27 V; t_a = 10 s)[7, 8]. In this case, j, the current density, is related to the growth of a thin (about 10 nm thickness) primary Ag(I) oxide layer[7, 8, 10, 11] and it obeys a linear j *vs* $t^{-1/2}$ relationship whose slope depends on the value of E_s. This linear relationship indicates that the primary Ag(I) oxide layer can be interpreted as a process controlled by a diffusion through the growing layer[11]. Accordingly, the following equation is obeyed:

$$j = P_4/t^{1/2} \qquad (1)$$

where $P_4 = z_i D^{1/2} c_i/\pi^{1/2}$, and z_i, D_i and c_i are the number of electrons per reacting species, the corresponding diffusion coefficient and the concentration of the species i, respectively. On the other hand, when the potential step coincides with the potential region of peak AI″, the process related to peaks AI′ and AI″ occur simultaneously. Correspondingly, the current transients exhibit a current plateau (Fig. 2a). As E_s increases, the height of the current plateau increases. The shape of these current transients is related to the nucleation and growth of islands of the secondary Ag(I) oxide layer[7] on top of the primary Ag(I) oxide layer.

On the other hand, when the electrode is preanodised for a time t_a in the potential region of peak AI′, to pre-form the primary Ag(I) oxide layer, the shape of the current transient (Fig. 2b) changes drastically and the charge involved is less than that derived from data shown in Fig. 2a. In this case, the current density initially decreases reaching a minimum value, j_m, at the time t_m, and later it increases sharply to reach a well defined maximum, j_M at the time t_M. Finally, the current decreases following a linear $t^{-1/2}$ dependence. As both t_a and E_s increase (Fig. 2c) the contribution of the initial falling current decreases and the value of j_M becomes much better defined. Thus, j_M increases and both t_m and t_M decrease as E_s is set more positively. For t_a = 600 s, one observes that the tails of the transients attain a common value which tends to become independent of E_s.

SEM micrographs of the electrode surface were obtained at E_a = 0.19 V, *ie* in the potential range of peak AI′, after anodising for t_a = 600 s. No crystal formation could be observed on the electrode at this potential value for X17000. On the other hand, when the potential was stepped from E_a = 0.19 V to E_s = 0.30 V, *ie* the potential region of peak AI″, a large number of crystals was seen on the electrode. The micrographs obtained after an anodisation time, $t_a = t_M$, (t_M = 1 s; E_s = 0.30 V), exhibited a large number of

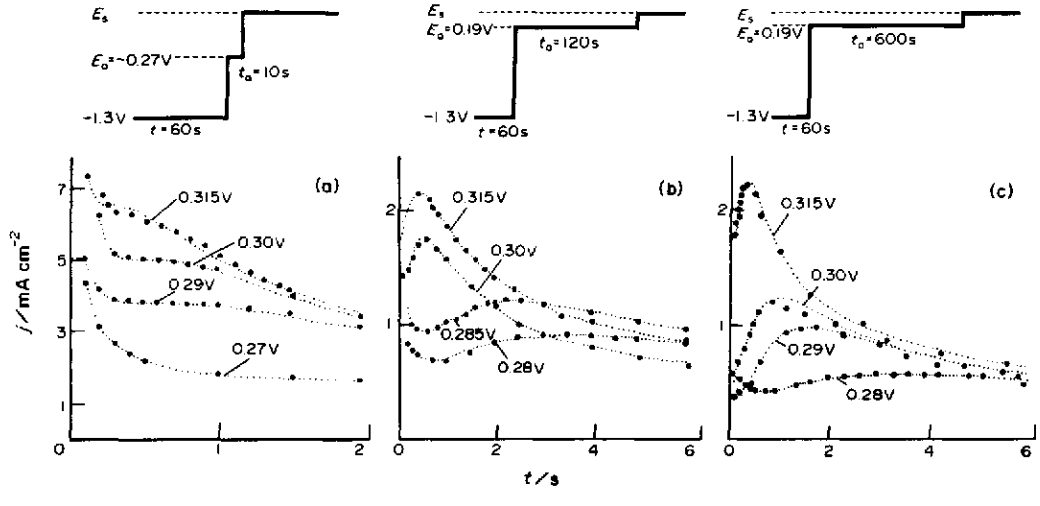

Fig. 2. (a) Current transients at constant E_s recorded for a polycrystalline Ag electrode in 0.1 M NaOH after applying to the electrode the following pretreatment: 60 s at −1.3 V to electroreduce the silver surface, immediately stepped to −0.27 V (double layer region) for 10 s, and finally held at E_s for current transients recording. (b) Current transients at constant E_s recorded for a polycrystalline Ag electrode in 0.1 M NaOH after applying to the electrode the following pretreatment: 60 s at −1.3 V, immediately stepped to 0.19 V (peak AI′) for t_a = 120 s, and finally stepped to E_s for current transients recording. (c) *idem* as (b) but t_a = 600 s. (■) experimental data, (....) calculated using equation (2).

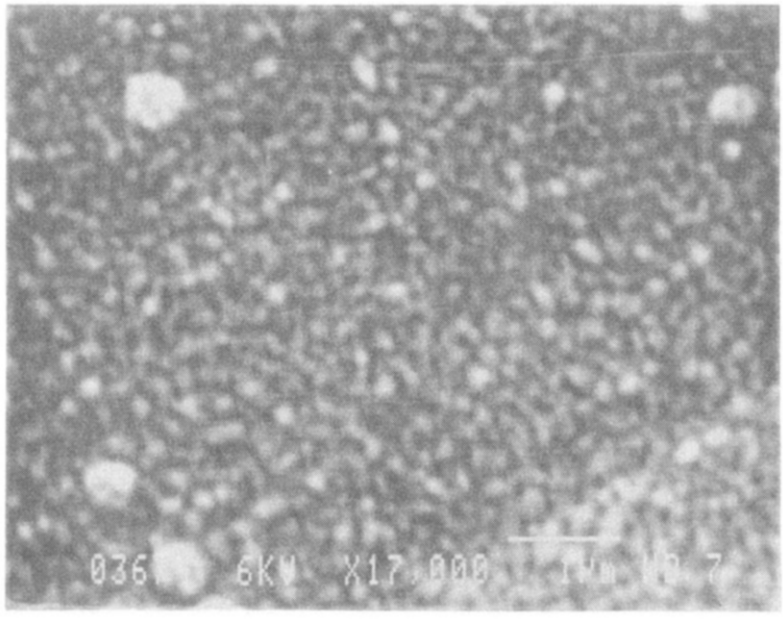

Fig. 3. SEM micrograph of the electrode surface after anodisation at 0.30 V for 70 s.

small hemispherical crystals, ($d = 50$ nm), together with a small number of large hemispherical crystals ($d = 300$ nm). The corresponding number density of crystals, N_s, was approximately 4×10^{10} cm^{-2}. Otherwise, for the same type of experiments, when the anodisation time at E_s lasted for 70 s, one observed an increase in the diameter of the small crystals and the development of agglomerates with a complex structure at sites where large hemispherical crystals were otherwise formed (Fig. 3). At this stage, a sharp decrease in the total number of crystals was found, a fact that can be attributed to a type of Ostwald ripening effect[11].

DISCUSSION

The formation of hemispherical crystals during the anodisation of silver in 0.1 M NaOH, the shape of the current transients for $t > t_m$, and the recently reported independence of the growth rate on potential[11], suggest that a nucleation and 3-D growth process under diffusion control operates during the electroformation of bulk Ag(I) oxide layer. To learn about quantitative kinetic aspects of this reaction, such as the nucleation rate, the corresponding rate constant, and the number of sites available for nucleation, a model for the complete electrochemical process must be considered.

Let us suppose that the bulk Ag(I) oxide layer electroformation includes the formation of the primary and the secondary layers on top of the Ag(I) oxygen-containing monolayer, the latter being in direct contact with the metal surface from the early stages of the process. Let us further assume that the electroformation of the Ag(I) secondary oxide layer involves the growth of spherical centers on the Ag(I) primary oxide layer as one can conclude from SEM micrographs (Fig. 3).The growth of each spherical center implies the diffusion of Ag^+ ions through the

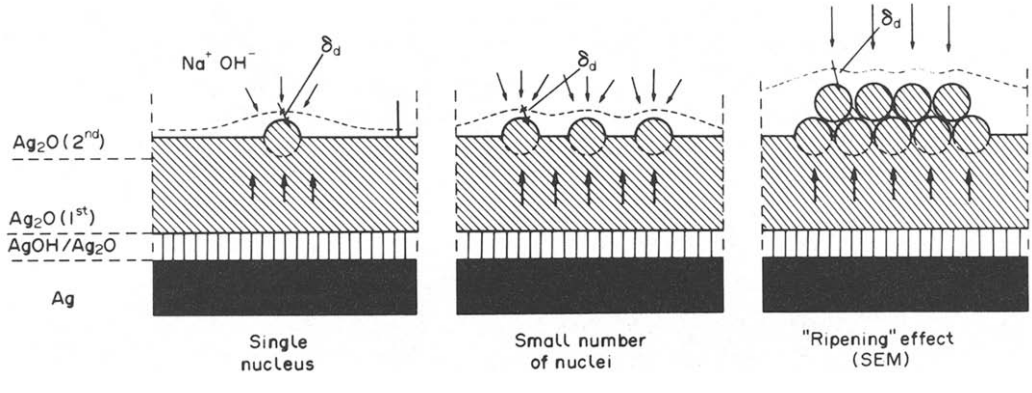

Fig. 4. Scheme of the model proposed for the nucleation and growth of the secondary Ag_2O layer. The thickness of the diffusional boundary layers for Ag^+ ions (δ_d) and for OH^- ions (δ'_d) are indicated. The arrows normal to the boundary layers indicate the direction of the diffusion field for each of those ions.

primary Ag(I) oxide layer, balanced by the radial diffusion of OH^- ions from the solution (Fig. 4). However, as the reaction proceeds, the overlap of diffusion zones from neighbouring nuclei results in a unidirectional diffusion field perpendicular to the electrode surface. The fact that the kinetic data obey equation (1)[7, 8, 10, 11] supports the idea that the growth mechanism is controlled by the diffusion of Ag(I) ions through the primary Ag(I) oxide layer. This assumption is supported by the fact that j remains independent of both solution stirring and OH^- ion concentration in solution[7, 12, 13]. Furthermore, this means that any OH^- ion concentration profile is fixed by the Ag(I) ion diffusion through the primary Ag(I) oxide layer.

The current transient equations, derived for nucleation and 3-D growth under diffusion control in[4], can be applied directly to the above model although cautiously because of the great number of assumptions involved in deriving those equations. In contrast to other data-processing techniques[3], in which only the product αN_0 or the value of N_0 is estimated the equations of[4] allow α and N_0 to be estimated separately. In fact, the entire bulk Ag(I) oxide layer current transient can be expressed in terms of two distinguishable contributions: (i) the initial falling current related to the growth of the primary Ag(I) oxide layer; (ii) the slower current response associated with the Ag(I) secondary oxide layer. The full equation is[4]:

$$j(t) = P_4/t^{1/2} + P_1/t^{1/2}\{1-\exp[-P_2 t + P_2/P_3 (1-\exp(P_3 t))]\} \quad (2)$$

where:

$$P_4 = zFD^{1/2}c/\pi^{1/2}, \quad (3)$$

$$P_1 = zFD'^{1/2}c'/\pi^{1/2}, \quad (4)$$

$$P_2 = K_e \pi D' N_0; \quad K_e = (8\pi M c'/\rho)^{1/2}, \quad (5)$$

$$P_3 = \alpha. \quad (6)$$

D and D', and c and c' are the diffusion coefficients and the bulk concentrations of the species involved in the electroformation of the primary and the secondary Ag(I) oxide layers, respectively. K_e denotes a proportionality constant. The first term in equation (2) accounts for the diffusional growth of the primary Ag(I) oxide layer, and the second term describes the nucleation and 3-D growth under diffusion control of the secondary Ag(I) oxide layer[4].

The current transients illustrated in Fig. 2 (dotted lines) were simulated by using equation (2) with the set of parameters assembled in Table 1. Those current transients obtained for $t_a = 600$ s exhibit excellent agreement between theory and experiment for the whole time window (15 s). In contrast, for $t_a = 0$ s, good curve fitting is obtained only for the first few seconds. In this case the departure between theory and experiment suggests that both Ag(I) oxide layers grow at the same time, that is, diffusional growth and nucleation and 3-D growth under diffusion-control contribute simultaneously to the electroformation process.

The values of P_4 furnish information about the growth of the primary Ag(I) oxide layer and its influence on the growth of the secondary Ag(I) oxide layer. Thus, for $t_a = 0$, large values of P_4 which tend to increase according to E_s are obtained. This fact indicates that the growth of the first Ag(I) oxide layer is then favoured. Otherwise, when $t_a \neq 0$, the previous formation of the primary Ag(I) oxide layer implies that its subsequent growth becomes hindered compared to $t_a = 0$. Then the values of P_4 appear to be independent of E_s and decrease on increasing t_a from 0 to 600 s (Table 1). Therefore, the flux of Ag^+ ions through the primary Ag(I) oxide layer which is required for building up the second Ag(I) oxide layer becomes hindered as the thickness of the primary Ag(I) oxide layer increases.

Other kinetic parameters provide further information about the nucleation and growth of the secondary Ag(I) oxide layer. Firstly, it should be noticed that P_1 becomes practically independent of the primary Ag(I)

Table 1. Parameters used for current transient fitting according to equation (2) as shown in Fig. 2 (dotted lines)

E_s/V	P_1/mA s$^{1/2}$ cm^{-2}	P_2/s	P_3/s^{-1}	P_4/mA s$^{1/2}$ cm^{-2}
$t_a = 0$ s				
0.270	1.45	1.68	0.31	1.46
0.280	2.00	1.79	1.11	1.63
0.290	2.67	2.92	1.19	1.82
0.300	2.94	3.58	1.99	2.10
0.310	3.03	4.46	4.97	2.09
$t_a = 120$ s				
0.280	1.32	1.17	1.63	0.32
0.285	1.42	1.81	2.19	0.38
0.300	1.23	4.47	3.70	0.36
0.315	1.06	5.29	16.6	0.50
$t_a = 600$ s				
0.280	1.35	0.36	1.64	0.22
0.290	1.36	1.67	1.65	0.10
0.300	1.32	2.60	3.19	0.13
0.315	1.23	7.29	6.59	0.35

oxide layer thickness. An estimation of the value of N_0 from equation (5) can be made provided that the values of c' and D' are available. The value of c' can be calculated from the following equation[14]:

$$r=(2D'c'Mt/\rho)^{1/2}, \quad (7)$$

where r is the radius of growing crystals, and t is the growth time. Then, by combining equations (4) and (7) one finds:

$$c^{1/2}=P_1(2M\pi t/\rho)^{1/2}/zFr. \quad (8)$$

Equation (8), for $t=1$ s, $r=2.5\times10^{-6}$ cm as derived from the SEM micrographs, $P_1=1.5$ mA $s^{1/2}$ cm^{-2}, $M=231$ g mol^{-1}, $z=1$ and $\rho=7.14$ g cm^{-3}, furnishes $c'=0.007$ mol cm^{-3}. This value can be introduced into equation (4) to obtain D' which results $D'=1\times10^{-11}$ cm^2 s^{-1}, a figure close to the diffusion coefficient of Ag^+ ions in bulk Ag_2O (4×10^{-12} cm^2s^{-1})[15]. This indicates that the transport of OH^- ions in the solution as controlling step for the growth of the secondary Ag(I) oxide layer should be definitely discarded[11].

By introducing c' and D' into equation (5) the value of N_0 in the range of overpotentials (η) covered by the present work is between 10^{10}–10^{11} cm^{-2}. The overpotential η is defined with respect to the reversible potential of the $Ag/Ag_2O/0.1$ NaOH electrode, $E_r=0.173$ V (*sce*), so that $\eta=E_s-E_r$. The corresponding ln N_0 *vs* η plots can be approximated as straightline relationships (Fig. 5) reaching a value of N_0 in the order of 10^{11} cm^{-2} which is independent of the age of the primary Ag(I) oxide layer (Figs 5a–c). Moreover, the slopes of the straight lines shown in Fig. 5 increase according to t_a. This means that the density of nucleation sites at the primary Ag(I) oxide layer increases with η. Nevertheless, at lower values of η, N_0 decreases as t_a increases.

According to the present model the maximum number of crystals related to the new phase, N_s, can be roughly estimated from the simple relationships[16, 17]:

$$N_s=\frac{1}{D't_m}, \quad (9)$$

or:

$$N_s=\left[\frac{\alpha N_0}{K_c D}\right]^{1/2}. \quad (10)$$

Thus, for $E_s=0.30$ V, from both equations N_s results 10^{11} cm^{-2}, a figure which is close to the number density of small crystals, N_s, in the SEM micrographs at t_M (Fig. 3). This agreement between the experimental and the theoretical crystal number density calculated throughout the nucleation and 3-D growth model under diffusion control contrasts with earlier reported data where the predicted values of N_s were several orders of magnitude smaller than the observed ones. The coincidence between N_s values found in the present work appears to be a firm argument in favour of the proposed model for the Ag(I) oxide phase electroformation.

The nucleation rate, α, which is included in the expression for P_3 (Table 1), increases as η is moved positively. This fact allows us to derive another important conclusion about the Ag(I) oxide phase electroformation. The nucleation stage can be considered as an electrochemical reaction instead of a chemical reaction, so that the supersaturation concentration of the soluble oxygen-containing species at the outer Ag(I) oxide layer depends on the following reaction:

$$Ag=Ag^+ + e^-. \quad (11)$$

Hence, the dependence of P_4 on η should be related to the η dependent concentration gradient of the Ag^+ ions which is established at the primary Ag(I) oxide layer. In this case n^*, the number of atoms or molecules constituting the critical nucleus, can be determined through the dependence of α on η.

According to the atomistic theory of electrochemical phase formation, both α and η are related through the equation[11]:

$$\alpha=k_{ff}\exp[-\phi(n^*)/kT]\exp[(n^*+\beta)ze\eta/kT], \quad (12)$$

where k_{ff} is a frequency factor, $\phi(n^*)$ accounts for the nucleus-ambient phase interaction, β is the transfer coefficient in the anodic direction, and k and T are the Boltzmann constant and the absolute temperature, respectively. The value of n^* comes out directly from the slope of the ln α *vs* η plot (Fig. 6). By taking $\beta=0.5$ and $z=1$, the value of n^* is found to be 1 for all t_a values (Figs 5a–c). This small number of atoms assigned to the critical nucleus justifies *post priori* the use of the atomistic approach[19]. Furthermore, the fact that α appears to be independent of t_a indicates that the time involved in converting an active site into a nucleus is not affected by the age of the primary Ag(I) oxide layer.

It should be noted, however, that attempts that were made to fit the current transients exhibiting well-defined maxima, by using only the second term of

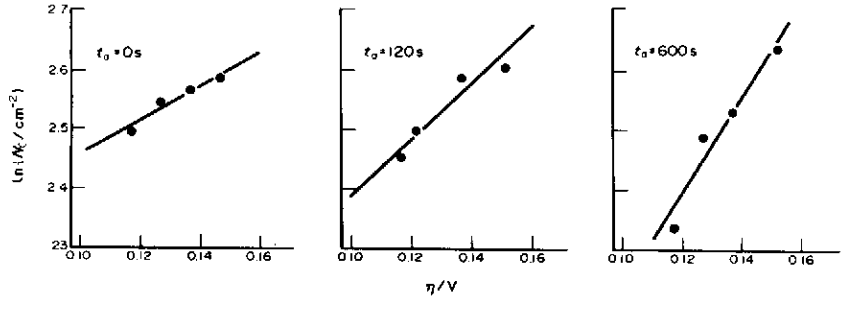

Fig. 5. ln N_0 *vs* η plots for different t_a.

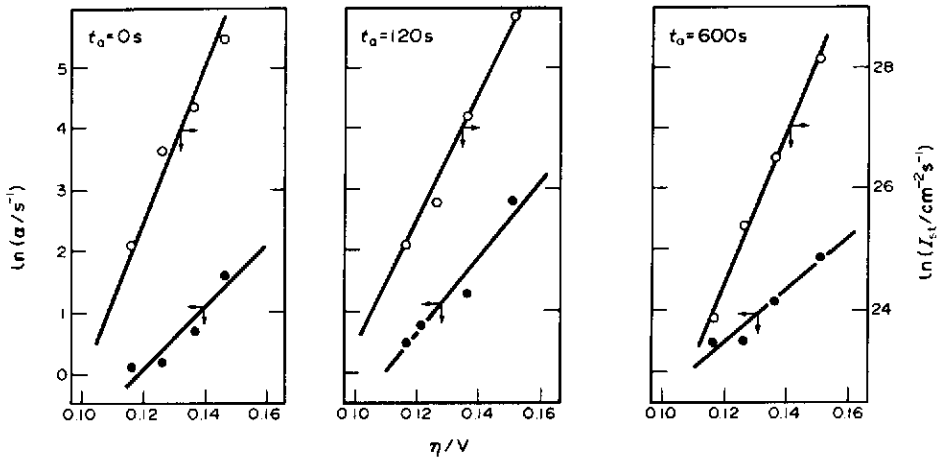

Fig. 6. ln α *vs* η and ln I_{st} *vs* η plots for different t_a.

equation (2), also yielded reasonable agreement between the experimental data and the theoretical equation. In these cases, no marked differences in the values of P_1 and P_2 were observed; but P_3 values were higher than those from the complete equation (2) (Table 2). This height, however, decreased as t_a increased, *ie* the current associated with the growth of the primary Ag(I) oxide layer decreased. It is quite evident that even small values of decreasing current transients related to that reaction can distort the resulting values of α. Decreasing current transients caused by adsorption or other processes are frequently observed before nucleation and 3-D growth transients. These can easily obscure the information about the nucleation and growth process in the rising part of the current transient. Inspection of P_3 data assembled in Table 2 reveals how this happens. However, one way to overcome this problem is to simulate the total transient to obtain the correct nucleation and growth parameters.

The stationary nucleation rate, I_{st}, is given by the relationship[20]:

$$I_{st} = \alpha N_o. \tag{13}$$

The overpotential dependence of I_{st} (Fig. 6) employed to determine n^* usually assumes that the dependence of N_o on η can be disregarded. However, this assumption cannot be justified in the case of the Ag(I) oxide layer electroformation (Fig. 5). If this were the case, the slope of the ln I_{st} *vs* η plot would furnish unlikely values of n^* such as, for $t_a = 0$ and $t_a = 120$ s, $n^* = 2$, and for $t_a = 600$ s, $n^* = 3$.

Table 2. Parameters used for current transient fitting with the second term of equation (2)

E_a/V	P_1/mA s$^{1/2}$ cm^{-2}	P_2/s	P_3/s^{-1}
$t_a = 120$ s			
0.285	1.82	1.36	14.0
0.300	1.63	3.00	29.5
0.315	1.53	6.43	263.4
$t_a = 600$ s			
0.290	1.47	1.45	2.63
0.300	1.48	1.9	9.56
0.315	1.60	5.86	20.87

In previous studies the decreasing current transients related to the Ag(I) oxide layer electroformation were assigned to a solid-diffusion controlled growth [8, 10, 12]. Therefore, nucleation and growth as the rate controlling step of this reaction was discarded, despite the fact that microscopic observations indicated the presence of isolated crystals growing on a flat basal oxide layer[10]. On the other hand, more recent work supplies evidence in favour of a nucleation and growth process as the rate controlling step of the Ag_2O phase electroformation[13, 7, 11, 21]. These discrepancies can be resolved by looking at the influence of the values P_1, P_2, P_3 and P_4 on the shape of the current transients in terms of equation (2) (Fig. 7). It is clear that a decrease in P_1 (Fig. 7a) masks the current maximum in the current transient. A similar effect is produced when the value of P_4 is increased (Fig. 7c), that is, when the contribution of the primary Ag(I) oxide layer becomes more important. Similar effects are produced when the values of P_2 (Fig. 7d) and P_3 (Fig. 7b) are increased. Although peaked current transients are often taken as diagnostic of nucleation and growth processes[7], one nevertheless has to be very cautious *not* to exclude nucleation and growth processes as rate controlling just because experimentally-observed transients lack peaks. Often, decreasing current transients may obscure nucleation processes. So, once again, simulation techniques appear as a valuable tool to discover the different stages participating in complex reaction pathways of phase change processes.

Finally, it is interesting to comment on the physical factors that govern the different growth modes of the Ag(I) oxide layer. After the first AgOH monolayer deposition, a thin primary Ag(I) oxide layer is formed, possibly epitaxially on the Ag substrate. However, at sufficiently positive potentials it is likely that the less hydrous anodic layer in contact with the metal surface corresponds to an epitaxial Ag_2O layer. This misfit between the thin Ag(I) oxide layer and the primary oxygen-containing monolayer should lead to a strain energy that acts as the driving force for cluster generation, *ie* the appearance of the secondary Ag(I) oxide

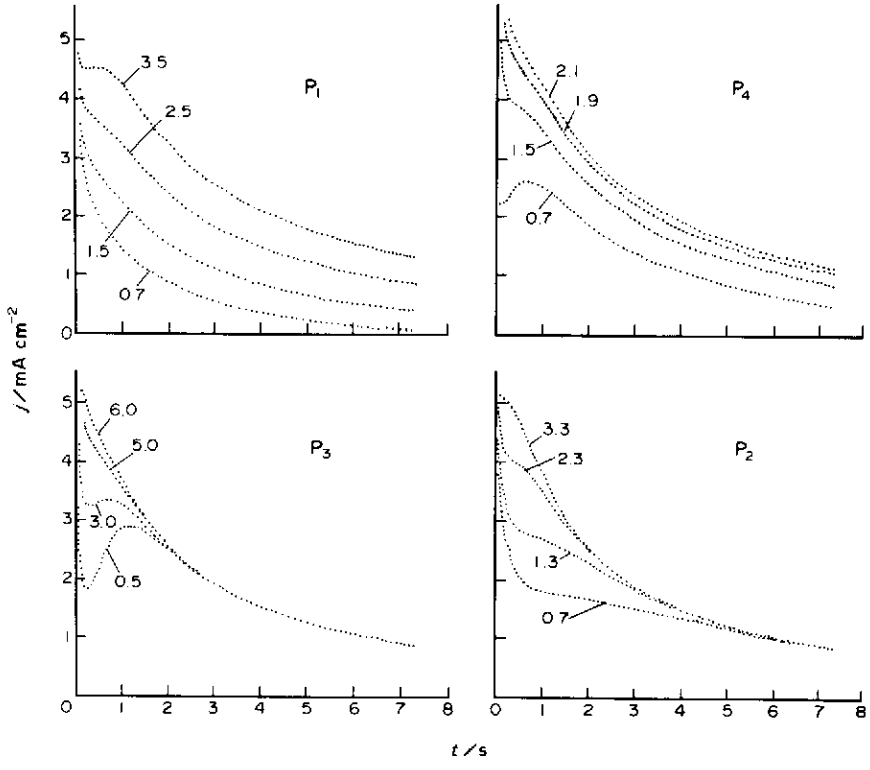

Fig. 7. The influence of the different P_i ($i=1, 2, 3, 4$) on the shape of the current transients obtained from equation (2).

layer[21]. For a degree of misfit (ϵ) greater than 0.1 a change from uniform film growth to Stranski–Krastanov growth (3-D clusters on the top of several layers of uniform film) should be expected. By using the relationship[21]:

$$\epsilon=\frac{a_d}{a_s}-1, \tag{14}$$

where a_d and a_s are the lattice parameters of the deposit ($a_d=4.73$ Å for Ag_2O) and the substrate ($a_s=4.08$ Å for Ag=AgOH) respectively, it results $\epsilon=0.16$. This figure explains the change in the mode of growth of the Ag(I) oxide layer on Ag electrodes in 0.1 M NaOH.

In conclusion, the processes participating in the formation of the secondary Ag(I) oxide layer can be summarized as follows:

$$Ag^+(\text{Metal}) \rightarrow Ag^+ \text{ (oxide/solution)}, \tag{15}$$

$$Ag^+ \text{ (oxide/solution)} + OH^- \text{ (solution)} \rightleftarrows \text{Ag(I) oxide (solution)}, \tag{16}$$

$$[\text{Ag(I)oxide}]_n + \text{Ag(I)oxide (solution)} \rightleftarrows [\text{Ag(I)oxide}]_{n+1}, \tag{17}$$

where n denotes the number of Ag(I) oxide units at the nucleus. According to the present study one concludes that the mass transport step (15) is rate determining for the Ag(I) oxide layer growth at constant potential. Simplified schemes for the formation of a single Ag(I) oxide nucleus, for the appearance of neighbouring nuclei with overlapping diffusion zones and for the agglomeration of nuclei (presumably equivalent to the ripening phenomenon as seen through the SEM), are illustrated in Fig. 4. In this case the different constituents of the anodic oxide layers, the direction of the diffusional fields for Ag^+ and OH^- ions, the diffusional boundary layer contours, and their overlapping according to the stage of the anodic process, are all indicated.

Acknowledgements—R.C.S. thanks the Consejo Nacional de Investigaciones Cientificas y Técnicas (Argentina) for a fellowship. This work was partially supported by the Regional Program for the Scientific and Technological Development of the Organization of the American States.

REFERENCES

1. M. Fleischmann and H. R. Thirsk, in *Advances in Electrochemistry and Electrochemical Engineering, Vol.* 3 (Edited by P. Delahay), p. 123, Interscience, New York (1961).
2. R. De Levie, in *Advances in Electrochemistry and Electrochemical Engineering*, Vol. 13 (Edited by H. Gerischer and C. W. Tobias), p. 1, Wiley, New York (1984).
3. B. Scharifker and G. Hills, *Electrochim. Acta* **28,** 879 (1983).
4. B. Scharifker and J. Mostany, *J. electroanal. Chem.* **177,** 13 (1984).
5. V. Tsakova and A. Milchev, *J. electroanal. Chem.* **235,** 237 (1987).
6. V. Tsakova and A. Milchev, *J. electroanal. Chem.* **235,** 249 (1987).

7. J. Gomez Becerra, R. C. Salvarezza and A. J. Arvia, *Electrochim. Acta* **33,** 1431 (1988).
8. J. M. Drogg, *J. electroanal. Chem.* **115,** 225 (1980).
9. M. Lopez Teijelo, J. R. Vilche and A. J. Arvia, *J. electroanal. Chem.* **131,** 331 (1982).
10. G. Briggs, M. Fleischmann, D. J. Lax and H. R. Thirsk *Trans. Faraday Soc.* **64,** 3120 (1968).
11. S. Meyer and R. Muller, *J. electrochem. Soc.* **135,** 2133 (1988).
12. J. Ambrose and R. Barradas, *Electrochim. Acta* **11,** 781 (1974).
13. M. Hepel and Tomkiewicz, *J. electrochem. Soc.* **131,** 1288 (1984).
14. G. Hills, D. Schiffrin and J. Thompson, *Electrochim. Acta* **11,** 657 (1974).
15. N. D. Rozenblyum, N. C. Bubyreva, V. I. Bukhareva and G. Z. Kazakevich, *Zh. fiz. Khim.* **40,** 2467 (1966).
16. J. Iacobs, *J. electroanal. Chem.* **247,** 135 (1988).
17. B. Scharifker, Acta cient. venez. **35,** 211 (1984).
18. F. Palmisano, E. Desimoni, L. Sabbatini and G. Torsi, *J. appl. Electrochem.* **9,** 517 (1979).
19. A. Milchev, S. Stoyanov and R. Kaischev, *Thin Solid Films* **22,** 255 (1974); **22,** 267 (1974).
20. A. Milchev and V. Tsakova, *Electrochim. Acta* **30,** 133 (1985).
21. B. G. Pound, D. D. MacDonald and J. W. Tomlinson, *Electrochim. Acta* **25,** 563 (1980).
22. M. H. Grabow and G. H. Gilmer, *Surf. Sci.* **194,** 333 (1988).